Excitonic polarons in confined systems

2004 J. Phys.: Condens. Matter 16 3981

(http://iopscience.iop.org/0953-8984/16/23/016)

INSTITUTE OF PHYSICS PUBLISHING JOURNAL OF PHYSICS: CONDENSED MATTER

J. Phys.: Condens. Matter **16** (2004) 3981–4000 PII: S0953-8984(04)76215-3

Excitonic polarons in confined systems

A Thilagam[1] **and A Matos-Abiague**[2]

[1] Department of Physics and Mathematical Physics, The University of Adelaide, South Australia 5005, Australia
[2] Max-Planck Institut für Mikrostrukturphysik, Weinberg 2, 06120 Halle, Germany

Received 12 February 2004
Published 28 May 2004
Online at stacks.iop.org/JPhysCM/16/3981
DOI: 10.1088/0953-8984/16/23/016

Abstract

We derive explicit analytical expressions for the ground state excitonic polaron (energy, effective mass) using the fractional-dimensional space formalism. Our results are shown to provide a wider overview of the character of the excitonic polaron than the analysis performed using integral dimensions only. We include a derivation of the energy difference between the 1s and 2s states as well as the phonon Lamb shift (energy difference between the 2p and 2s states) in simple analytical forms. Our results compare well with experimental data and earlier theoretical estimates for a variety of different material systems. We extend the fractional-dimensional model to analyse excitonic polarons in coupled double quantum wells and quantum disc systems.

1. Introduction

The quantum effects of low-dimensional electronic systems have attracted much attention in recent years. On the experimental side, this trend towards miniaturization is driven by applications which include electronic devices based on parallel and perpendicular transport, optical devices [1], quantum computation, and quantum information [2]. On the theoretical side, there are efforts to improve the understanding of many phenomena in these restricted geometries [3, 4], even though significant development has been achieved in experimental techniques such as MBE growth and synthesis and optical characterization of quantum wells (QWs) and superlattices.

The polaron problem, first initiated by Landau [5], has since then been studied extensively [6–8] and has provided an exemplary system for testing new non-perturbative methods [9]. It has also been extended to investigate the properties of other systems like bipolarons [10] and excitonic polarons [8, 11–15]. Our aim in this paper is to simplify the large computational efforts usually demanded within the standard methods, in order to study the properties of excitonic polarons in a simple, accurate, and comprehensive physical model. The model is based on the fractional-dimensional space approach [16, 17], a formalism that provides an elegant short path to tackling the geometrical complexities of low-dimensional

systems. Using this technique, we are able to provide a clear physical insight into the properties of the excitonic polaron. We also extend the proposed theoretical treatment to study the energy difference between the 1s and 2s as well as between 2p and 2s states (phonon Lamb shift) in QWs and excitonic properties in coupled double quantum wells and quantum disc systems.

Even though non-integer dimensions are not easily conceivable, the fractional-dimensional space approach has introduced a new, alternative and powerful way for calculating exciton binding energies in quantum wells [17–21] which otherwise have appeared unmanageable by conventional approaches unless numerical calculations are performed [22]. In this scheme, the real confined 'exciton + quantum well', 'exciton + phonon + quantum well' or 'exciton + electric (magnetic) field + quantum well' system is mapped onto an effective fractional-dimensional space in which the composite exciton system behaves in an unconfined manner and in which the fractional dimension is essentially related to the degree of confinement of the actual system. Such an approach introduces simplicity and utility and has since been used in the investigation of several important processes in QWs such as Pauli blocking effects [23], impurity and donor states [24, 25], excitonic characteristics in magnetic fields [26, 27], Stark effects in weak electric fields [28], modelling of refractive index [29], exciton–exciton interaction [30], polarons [31], exciton linewidth properties [32], optical effects in a microcavity [33], and coherent states [34]. These studies have highlighted the useful and important role of the dimensionality (from now on denoted by α) which interpolates from 2 in an exact two-dimensional system (e.g., infinite potential quantum well with zero well width) to 3 in an exact three-dimensional system (e.g., infinitely wide quantum well). In this regard, the fractional-dimensional space approach has provided a comprehensive understanding of physical properties in low-dimensional systems.

The paper is organized as follows. In section 2, we present the theory needed to evaluate the energy of the excitonic polaron within the framework of the fractional-dimensional space approach. Analytical expressions of the excitonic polaron corrections (energy, effective mass) are derived in section 3, and the corresponding expression for the binding energy of an exciton interacting with phonons is evaluated in section 4. In section 5, we extend the theory developed in section 2 to obtain analytical expressions for the energy difference between the 1s and 2s excitonic polaron states as well as for the corresponding 2p–2s energy difference (phonon Lamb shift). In section 6, we perform a comparative study of our fractional-dimensional results with available experimental data and other theoretical estimates for a variety of different material systems. In sections 7 and 8 we extend the calculations to study the properties of excitonic polarons in coupled double quantum wells and quantum disc systems, respectively. Finally, conclusions are summarized in section 9.

2. Ground state of the excitonic polaron

One of the difficulties in solving the problem of exciton–phonon interaction is that the Hamiltonian consisting of exciton, phonon and exciton–phonon interaction energy operators is not diagonal, either in k-space or in real crystal space. Approximate methods are generally used [6] to solve the problem. If the exciton–phonon interaction is weak enough, perturbation theory can be used to obtain the energy eigenvalues and eigenfunctions of an exciton interacting with phonons. Another technique involves diagonalization of the Hamiltonian as best as possible and then the remaining off-diagonal terms are treated as perturbations. We will adopt the second method in the present section.

The Hamiltonian $\hat{H}_{\mathrm{T}}$ that describes a Wannier exciton interacting with phonons in a fractional-dimensional space (α-D space) consists of the exciton energy operator $\hat{H}_{\mathrm{ex}}^{\alpha\mathrm{D}}$, the

phonon energy operator $\hat{H}_{\rm ph}$, and the exciton–phonon interaction energy operator $H_{\rm ex-ph}^{{\rm op}\,\alpha{\rm D}}$:

$$\hat{H}_{\rm T} = \hat{H}_{\rm ex}^{\alpha{\rm D}} + \hat{H}_{\rm ph} + \hat{H}_{\rm ex-ph}^{{\rm op}\,\alpha{\rm D}}, \tag{1}$$

where the superscript αD refers to the exciton in a space characterized by the fractional dimension α and op specifies that in the present work we consider exciton interaction with optical phonons only. Each term of equation (1) is defined as follows:

$$\hat{H}_{\rm ex}^{\alpha{\rm D}} = \sum_{\mathbf{K},\nu} E_{\nu}^{\rm ex}(\mathbf{K}) B_{\mathbf{K},\nu}^{\dagger} B_{\mathbf{K},\nu}, \tag{2}$$

where the exciton energy is determined by

$$E_{\nu}^{\rm ex}(\mathbf{K}) = E_{\rm g}^{\alpha{\rm D}} + \frac{\hbar^2\mathbf{K}^2}{2M_{\rm ex}^*} - \frac{R_y}{\left(\nu + \frac{\alpha-3}{2}\right)^2}, \tag{3}$$

and $E_{\rm g}^{\alpha{\rm D}}$ is the fractional-dimensional band gap, $\mathbf{K}$ denotes the exciton pseudo-wavevector, $M_{\rm ex}^*$ represents the effective exciton mass which is assumed to be isotropic in the fractional-dimensional space, $\nu = 1, 2, \ldots$ is the principal quantum number of the exciton internal state, $B_{\mathbf{K},\nu}^{\dagger}$ and $B_{\mathbf{K},\nu}$ are the excitonic creation and annihilation operators, respectively, and R_y is the effective Rydberg. It is to be noted that the last term in equation (3) represents the binding energy of a fractional-dimensional exciton [18] without taking account of the interaction with phonons. We remark that the fractional-dimensional band gap $E_{\rm g}^{\alpha{\rm D}}$ corresponds to the effective fractional-dimensional environment in which the excitonic polaron remains in an unconfined fashion. The effective fractional-dimensional system is then used to map the real confined excitonic polaron system. Consequently, for practical purposes, and in order to guarantee the mapping between both the real and the effective systems, the fractional-dimensional band gap $E_{\rm g}^{\alpha{\rm D}}$ has to be renormalized to an appropriate value. For the case of QWs it has been shown that $E_{\rm g}^{\alpha{\rm D}} = E_{\rm c} + E_{\rm v} + E_{\rm g}^{\rm 3D}$ (see [21]), $E_{\rm g}^{\rm 3D}$ being the usual (three-dimensional) bulk gap of the actual system and $E_{\rm v}$ ($E_{\rm c}$) the confining (positive) energy of the top (bottom) of the first valence (conduction) subband.

$\hat{H}_{\rm ph}$ is the optical phonon energy operator given by

$$\hat{H}_{\rm ph} = \sum_{\mathbf{q}} \hbar\omega_{\mathbf{q}} b_{\mathbf{q}}^{\dagger} b_{\mathbf{q}}, \tag{4}$$

where, for simplification, we have omitted the zero point energy term.

We define the α-dimensional exciton–phonon interaction involving longitudinal optical phonons by the Fröhlich type Hamiltonian [32]:

$$H_{\rm ex-ph}^{{\rm op}\,\alpha{\rm D}} = \sum_{\mathbf{K},\mathbf{q},\lambda,\nu} V_{\lambda,\nu}^{\alpha}(\mathbf{q}) B_{\mathbf{K}+\mathbf{q},\nu}^{\dagger} B_{\mathbf{K},\lambda}(b_q + b_q^{\dagger}) \tag{5}$$

where $\mathbf{q}$ represents the phonon wave pseudovector, λ and ν denote internal quantum numbers of the exciton states, and b_q and $b_q^{\dagger}$ refer to the phonon annihilation and creation operators, respectively. It is to be noted that the use of pseudo-wavevectors ($\mathbf{K}$ and $\mathbf{q}$) and hence a k-space formalism in a fractional-dimensional space is well documented in the literature (see [35] and references therein). Unlike in conventional approaches, these pseudovector states occupy the space of non-integer dimensionality. Accordingly, the summation over $\mathbf{K}$ and $\mathbf{q}$ can be converted to an integral over positive $|\mathbf{K}|$ or $|\mathbf{q}|$, as will be shown in section 3.

The matrix element $V_{\lambda,\nu}^{\alpha}(\mathbf{q})$ that appears in equation (5) is given by

$$V_{\lambda,\nu}^{\alpha}(\mathbf{q}) = \int_{\alpha{\rm D}} {\rm d}\mathbf{r}\, \psi_{\nu}^{\dagger}(\mathbf{r}) \psi_{\lambda}(\mathbf{r}) V_{\mathbf{q}}^{\alpha} \left[\exp(-{\rm i}\gamma_{\rm e}\mathbf{q}\cdot\mathbf{r}_{\rm e}) - \exp({\rm i}\gamma_{\rm h}\mathbf{q}\cdot\mathbf{r}_{\mathbf{h}})\right], \tag{6}$$

where

$$\gamma_{\rm e} = \frac{m_{\rm e}^*}{(m_{\rm e}^* + m_{\rm h}^*)}, \qquad \gamma_{\rm h} = \frac{m_{\rm h}^*}{(m_{\rm e}^* + m_{\rm h}^*)}, \tag{7}$$

and

$$|V_{\mathbf{q}}^{\alpha}|^2 = \frac{\Gamma\left[\frac{(\alpha-1)}{2}\right](4\pi)^{(\alpha-1)/2} e^2 \hbar\omega}{2\Omega^{\alpha} q^{\alpha-1}} \left(\frac{1}{\varepsilon_\infty} - \frac{1}{\varepsilon_0}\right). \tag{8}$$

In the equations above, ε_∞ and ε_0 are the high- and low-frequency values of the dielectric function of the well material, $m_{\rm e}^*$ and $m_{\rm h}^*$ are the respective electron and hole effective masses, and ω is the frequency of the LO phonons. In equation (8), we have neglected the LO-phonon dispersion by assuming that $\hbar\omega_{\mathbf{q}} \approx \hbar\omega$. Ω^{α} in equation (8) is the fractional-dimensional volume of the crystal to which Born–Von Karman periodicity conditions are applied. The form of $V_{\mathbf{q}}^{\alpha}$ as given in equation (8) was derived in [31] by using the fractional-dimensional Fourier transform [16] of the Coulomb-like potential that basically characterizes the electron (or hole) interaction with the lattice. It is to be noted that equation (8) reduces to the well established forms in both the exact 2D and 3D limits.

For $\lambda = \nu = 1$s, the matrix element $V_{1{\rm s},1{\rm s}}^{\alpha}(\mathbf{q})$ in equation (6) is evaluated using the 1s state of an exciton in an αD space:

$$\psi_{1{\rm s}}(r) = F(\alpha) \exp\left[-\frac{2}{\alpha - 1}\frac{r}{a_{\rm B}}\right]. \tag{9}$$

One then arrives at the following expression [32]:

$$V_{1{\rm s},1{\rm s}}^{\alpha}(\mathbf{q}) = \left(\frac{\Gamma\left[\frac{(\alpha-1)}{2}\right](4\pi)^{(\alpha-1)/2} e^2 \hbar\omega}{2\Omega^{\alpha} q^{\alpha-1}}\right)^{1/2} \left(\frac{1}{\varepsilon_\infty} - \frac{1}{\varepsilon_0}\right)^{1/2} \times \left[\frac{1}{(1+\beta_h^2(\alpha))^{(\alpha+1)/2}} - \frac{1}{(1+\beta_{\rm e}^2(\alpha))^{(\alpha+1)/2}}\right], \tag{10}$$

where

$$\beta_{\rm h}(\alpha) = \frac{\gamma_{\rm h}|\mathbf{q}|}{2}\left(\frac{\alpha-1}{2}\right) a_{\rm B}, \qquad \beta_{\rm e}(\alpha) = \frac{\gamma_{\rm e}|\mathbf{q}|}{2}\left(\frac{\alpha-1}{2}\right) a_{\rm B}, \tag{11}$$

and $a_{\rm B}$ is the three-dimensional Bohr radius of the exciton. The term $F(\alpha)$ in equation (9) can be easily obtained from the normalization of the 1s exciton wavefunction [17]. In what follows we omit, for brevity, the internal quantum numbers ($\lambda = \nu = 1$ s) in the labels of the excitonic creation and annihilation operators.

One can notice that the interaction operator $H_{\rm ex-ph}^{{\rm op}\,\alpha{\rm D}}$ in equation (5) is not diagonal with respect to exciton or phonon operators and, consequently, the total Hamiltonian $\hat{H}_{\rm T}$ in equation (1) is also non-diagonal. We will therefore diagonalize $\hat{H}_{\rm T}$, as best as possible, by applying the unitary transformation [36] $U_{\rm ex}$:

$$U_{\rm ex} = {\rm e}^{{\rm i}S}, \tag{12}$$

where S is given by

$$S = \sum_{\mathbf{K},\mathbf{q}} B_{\mathbf{K}+\mathbf{q}}^{\dagger} B_{\mathbf{K}} \left(f_{\rm ex}^*(\mathbf{K},\mathbf{q}) b_{-q}^{\dagger} + f_{\rm ex}(\mathbf{K},\mathbf{q}) b_q\right), \tag{13}$$

and the function $f_{\rm ex}(\mathbf{K},\mathbf{q})$ is determined through the process of diagonalization. The series of expansion needed to transform the Hamiltonian can be written as

$$U_{\rm ex}^{-1}\hat{H}U_{\rm ex} = \hat{H}_0 + ({\rm i}[\hat{H}_0, S] \pm \hat{H}_{\rm ex-ph}^{{\rm op}\,Q2{\rm D}}) + {\rm i}\left[\left(\tfrac{1}{2}{\rm i}[\hat{H}_0, S] \pm \hat{H}_{\rm ex-ph}^{{\rm op}\,Q2{\rm D}}\right), S\right] \pm \cdots, \tag{14}$$

where $\hat{H}_0 = \hat{H}_{\rm ex}^{\alpha {\rm D}} + \hat{H}_{\rm ph}$. Using equations (2), (4), (5), (12) and (13) in (14), the function $f_{\rm ex}$ is found to be

$$f_{\rm ex}(\mathbf{K},\mathbf{q}) = \frac{V_{1{\rm s},1{\rm s}}^{\alpha}(\mathbf{q})}{E_{1{\rm s}}^{\rm ex}(\mathbf{K}+\mathbf{q}) - E_{1{\rm s}}^{\rm ex}(\mathbf{K}) - \hbar\omega}, \tag{15}$$

with a similar expression for $f_{\rm ex}^{*}(\mathbf{K},\mathbf{q})$. The transformed Hamiltonian $\hat{H}^{\rm T} = U_{\rm ex}^{-1}\hat{H}U_{\rm ex}$ is thus obtained as

$$\hat{H}_{\rm T} = \hat{H}_{\rm ex}^{\alpha {\rm D}} + \hat{H}_{\rm ph} + \hat{H}_{\rm ex-ph}^{{\rm T\ op}\ \alpha {\rm D}} + \hat{H}_I', \tag{16}$$

where $\hat{H}_{\rm ex-ph}^{{\rm T\ op}\ \alpha {\rm D}}$ is given by

$$\hat{H}_{\rm ex-ph}^{{\rm T\ op}\ \alpha {\rm D}} = \sum_{\mathbf{K}}\sum_{\mathbf{K}',\mathbf{q}}\left\{|V_{1{\rm s},1{\rm s}}^{\alpha}(\mathbf{q})|^2\left[\frac{1}{E_{1{\rm s}}^{\rm ex}(\mathbf{K}+\mathbf{q}) - E_{1{\rm s}}^{\rm ex}(\mathbf{K}) - \hbar\omega}\right.\right.$$
$$\left.\left. - \frac{1}{E_{1{\rm s}}^{\rm ex}(\mathbf{K}+\mathbf{q}) - E_{1{\rm s}}^{\rm ex}(\mathbf{K}) + \hbar\omega}\right] B_{\mathbf{K}}^{\dagger} B_{\mathbf{K}+\mathbf{q}} B_{\mathbf{K}'+\mathbf{q}}^{\dagger} B_{\mathbf{K}'}\right\}. \tag{17}$$

It is worth noting that the transformed Hamiltonian in equation (16), the function $f_{\rm ex}(\mathbf{K},\mathbf{q})$ (see equation (15)), has been obtained such that the non-diagonalized term $\hat{H}_I'$ is expected to contribute with a small energy correction to the excitonic polaron even in the intermediate coupling regime. The neglect of this term in the weak and intermediate coupling regimes is well justified, as will be shown in section 6, where comparisons are made with experimental data and earlier theoretical estimates for a variety of different material systems.

The state vector of an α-dimensional excitonic polaron can be represented by $|\mathbf{K}; n(\mathbf{q})\rangle = B_{\mathbf{K}}^{\dagger}|0; n(\mathbf{q})\rangle$ (with $|0; n(\mathbf{q})\rangle = |0\rangle \times |n(\mathbf{q})\rangle$), where $|0\rangle$ is the vacuum state vector of excitons and $|n(\mathbf{q})\rangle = |n_{\mathbf{q}_1}, n_{\mathbf{q}_2}, \ldots\rangle$ is the α-dimensional optical phonon state pseudovector characterized by the occupation number $n_{\mathbf{q}}$ of phonons with wave pseudovector $\mathbf{q}$. By setting $n_{\mathbf{q}} = 0$, the ground state of the excitonic polaron is then evaluated as

$$E_{\rm ex-pol}^{1{\rm s}} = \langle n(\mathbf{q}), \mathbf{K}|U_{\rm ex}^{-1}\hat{H}_{\rm ex-ph}^{{\rm T\ op}\ \alpha {\rm D}}U_{\rm ex}|\mathbf{K}, n(\mathbf{q})\rangle$$
$$= E_{\rm g} + \frac{\hbar^2\mathbf{K}}{2M_{\rm ex}^{*}} - \frac{R_y}{\left(1+\frac{\alpha-3}{2}\right)^2} - I^{\rm ex}(\mathbf{K}) + \langle 0; \mathbf{K}|\hat{\mathbf{H}}_I'|\mathbf{K}; 0\rangle, \tag{18}$$

where

$$I^{\rm ex}(\mathbf{K}) = \sum_{\mathbf{q}}\left\{|V_{1{\rm s},1{\rm s}}^{\alpha}(\mathbf{q})|^2\left[\frac{1}{E_{1{\rm s}}^{\rm ex}(\mathbf{K}+\mathbf{q}) - E_{1{\rm s}}^{\rm ex}(\mathbf{K}) - \hbar\omega} - \frac{1}{E_{1{\rm s}}^{\rm ex}(\mathbf{K}+\mathbf{q}) - E_{1{\rm s}}^{\rm ex}(\mathbf{K}) + \hbar\omega}\right]\right\}. \tag{19}$$

It can be easily shown that $\langle 0; \mathbf{K}|\hat{\mathbf{H}}_I'|\mathbf{K}; 0\rangle = 0$ so that the first order contribution of $\hat{H}_I'$ to the ground state energy is zero, although this may not be true for higher energy states with non-zero values of $n_{\mathbf{q}}$.

3. Evaluation of $I^{\rm ex}(\mathbf{K})$ in a fractional-dimensional space

The term $I^{\rm ex}(\mathbf{K})$ in equation (19) can be evaluated by transforming the discrete sum over the phonon wave pseudovector $\mathbf{q}$ into a spatial integral using the relation

$$\sum_{\mathbf{q}} \longrightarrow \frac{\Omega^{\alpha}}{(2\pi)^{\alpha}}\frac{2\pi^{(\alpha-1)/2}}{\Gamma[\frac{\alpha-1}{2}]}\int_{\alpha {\rm D}} q^{\alpha-1}(\sin\theta)^{\alpha-2}\,{\rm d}q\,{\rm d}\theta. \tag{20}$$

Assuming parabolic bands, $I^{\rm ex}(\mathbf{K})$ in equation (19) can be rewritten as

$$I^{\rm ex}(\mathbf{K}) = \sum_{\mathbf{q}} |V^{\alpha}_{1{\rm s},1{\rm s}}(\mathbf{q})|^2 \left[\frac{1}{\frac{\hbar^2 q^2}{2M^*_{\rm ex}} - \hbar\omega + \frac{\hbar^2 \mathbf{K}\cdot\mathbf{q}}{M^*_{\rm ex}}} - \frac{1}{\frac{\hbar^2 q^2}{2M^*_{\rm ex}} + \hbar\omega + \frac{\hbar^2 \mathbf{K}\cdot\mathbf{q}}{M^*_{\rm ex}}} \right]. \tag{21}$$

Equation (21) can be simplified by considering that $\left(\hbar\omega + \frac{\hbar^2 q^2}{2M^*_{\rm ex}}\right) \gg \frac{\hbar^2}{M^*_{\rm ex}}\mathbf{K}\cdot\mathbf{q}$ for excitons present near the band edge [37] and using the identity

$$\int_0^{\pi} \frac{(\sin\theta)^u}{a + b\cos\theta}\,{\rm d}\theta = \frac{\sqrt{\pi}\Gamma[\frac{1+u}{2}]}{a\Gamma[1+\frac{u}{2}]}\,{}_2F_1\left(\frac{1}{2}, 1, 1+\frac{u}{2}, \frac{b^2}{a^2}\right), \tag{22}$$

where the hypergeometric function ${}_2F_1(\frac{1}{2}, 1, 1+\frac{u}{2}, x) \approx 1 + \frac{x}{2(1+\frac{u}{2})}$ for small x. We thus obtain $I^{\rm ex}(\mathbf{K}) \approx I^{\rm ex}_1 + I^{\rm ex}_2(\mathbf{K})$ with

$$I^{\rm ex}_1 = -\eta_{\rm ex} M_1(\alpha, \gamma_{\rm e}, \gamma_{\rm h})\hbar\omega \tag{23}$$

and

$$I^{\rm ex}_2 = \left(\frac{\hbar^2 K^2}{2M^*_{\rm ex}}\right)\eta_{\rm ex} M_2(\alpha, \gamma_{\rm e}, \gamma_{\rm h}), \tag{24}$$

where $M_1(\alpha, \gamma_{\rm e}, \gamma_{\rm h})$ and $M_2(\alpha, \gamma_{\rm e}, \gamma_{\rm h})$ are functions that will be explicitly determined, and $\eta_{\rm ex}$ represents the dimensionless exciton–phonon coupling constant:

$$\eta_{\rm ex} = \left(\frac{2M^*_{\rm ex}\omega}{\hbar}\right)^{1/2} \frac{e^2}{2\hbar\omega}\left(\frac{1}{\varepsilon_\infty} - \frac{1}{\varepsilon_0}\right). \tag{25}$$

It is worth noting that careful attention has to be given to the evaluation of the integrals in $I^{\rm ex}_1$ and $I^{\rm ex}_2(\mathbf{K})$ due to the divergence which occurs at $E^{\rm ex}_{1{\rm s}}(\mathbf{K}+\mathbf{q}) - E^{\rm ex}_{1{\rm s}}(\mathbf{K}) = \hbar\omega$. A suitable way to deal with this problem is to separate the region of integration into two sub-intervals [38] and choose the division to be at the point of divergence. An accurate integral can thus be obtained as imaginary and divergent terms cancel each other. The following integral becomes useful when using this method of integration over the region of singularity:

$$\int_h^k (x^2 - a)^{-1}(bx^2 + 1)^{-u}\,{\rm d}x$$
$$= -\frac{h}{a}F_1\left(\frac{1}{2}; 1, u; \frac{3}{2}; \frac{h^2}{a}, -bh^2\right) - \frac{k}{a}F_1\left(\frac{1}{2}; 1, u; \frac{3}{2}; \frac{k^2}{a}, -bk^2\right), \tag{26}$$

where the function F_1 represents one of the four hypergeometric functions in two variables introduced by Appell [39] and defined as

$$F_1(a; b_1, b_2; c; x, y) = \sum_{m=0}^{\infty}\sum_{n=0}^{\infty} (a)_{m+n}(b_1)_m \frac{(b_2)_n}{m!n!(c)_{m+n}} x^m y^n, \tag{27}$$

$(a)_n$ being the standard Pochhammer symbol $(a)_n = \frac{\Gamma(a+n)}{\Gamma(a)} = a(a+1)\cdots(a+n-1)$ with $(a)_0 = 1$.

Accurate numerical values of $I^{\rm ex}_1$ and $I^{\rm ex}_2(\mathbf{K})$ can thus be computed with standard packages that provide direct values of the Appell function F_1 for given values of its parameters. However, in order to obtain $M_1(\alpha, \gamma_{\rm e}, \gamma_{\rm h})$ and $M_2(\alpha, \gamma_{\rm e}, \gamma_{\rm h})$ as explicit analytical functions, we terminate the series expansion of F_1 in y (see equation (27)) at the third term. As $0 \leqslant \gamma_{\rm e}\gamma_{\rm h} \leqslant \frac{1}{4}$, this approximation is valid for $\left(\frac{a_{\rm B}}{4R_{\rm ex}}\right) \leqslant 1$, a condition that is fulfilled by a wide range of materials commonly used as constituents in nanostructured systems. We then obtain $M_1(\alpha, \gamma_{\rm e}, \gamma_{\rm h})$ and $M_2(\alpha, \gamma_{\rm e}, \gamma_{\rm h})$ as

$$M_1(\alpha, \gamma_{\rm e}, \gamma_{\rm h}) \approx \frac{\sqrt{\pi}\Gamma[\frac{\alpha}{2} - \frac{1}{2}]}{2\Gamma[\frac{\alpha}{2}]} D(\alpha, a_{\rm B}, R_{\rm ex}, \gamma_{\rm e}, \gamma_{\rm h}) \tag{28}$$

and

$$M_2(\alpha, \gamma_e, \gamma_h) \approx \frac{\sqrt{\pi}\Gamma[\frac{\alpha}{2} - \frac{1}{2}]}{8\Gamma[\frac{\alpha}{2} + 1]} D(\alpha, a_B, R_{ex}, \gamma_e, \gamma_h), \tag{29}$$

where

$$D(\alpha, a_B, R_{ex}, \gamma_e, \gamma_h) = \left[1 - \frac{1}{C^{1+\alpha}} + \left(\frac{1+\alpha}{2(\alpha-1)}\right)\left(\frac{a_B}{4R_{ex}}\right)^2 \left(\gamma_e^2 + \gamma_h^2 - 2C^{-2-\alpha}\mu\right)\right], \tag{30}$$

$\mu = \gamma_e\gamma_h$, $C = \frac{1}{2\mu} - 1$, and $R_{ex} = \sqrt{\frac{\hbar}{2M_{ex}^*\omega}}$. One can notice that in the limit $m_e = m_h$ (i.e., $\gamma_e = \gamma_h$) the centre of mass and the centre of charge coincide. Consequently, the screening between the electron and hole becomes very effective and the coupling with the phonons is minimal. In agreement with this situation, one can easily verify that when $\gamma_e = \gamma_h$ both M_1 and M_2 vanish, as expected. Another interesting limiting case occurs when either the electron or the hole mass vanishes and the terms associated with a_B are neglected. In that case, as one can expect, the expressions for M_1 and M_2 in equations (28) and (29) reduce to the corresponding ones referred to the single polaron case [31].

Within the framework of our model the ground state energy of the excitonic polaron can then be written as

$$E_{ex-pol}^{1s} = \frac{\hbar^2\mathbf{K}^2}{2M_{ex}^*}\left[1 - \eta_{ex}M_2(\alpha, \gamma_e, \gamma_h)\right] - \frac{4R_y}{(\alpha-1)^2} + E_g^{\alpha D} - \eta_{ex}\hbar\omega M_1(\alpha, \gamma_e, \gamma_h), \tag{31}$$

where the first and last terms in equation (31) represent the kinetic energy and the energy gap shift, respectively. From equation (31) it follows that the effective mass of an α-dimensional excitonic polaron is given by $M_p^* = \frac{M_{ex}^*}{1-\eta_{ex}M_2(\alpha,\gamma_e,\gamma_h)}$.

As can be appreciated from equations (28)–(31), the ground state energy of the excitonic polaron is an explicit function of $\sigma = m_e/m_h$ (the ratio of electron to hole mass), the LO-phonon energy, the ratio of the exciton Bohr radius to the excitonic polaron radius (a_B/R_{ex}), the exciton coupling constant (η_{ex}), and the dimensionality α. In order to gain some physical insight into the dependence of the ground state energy E_{ex-pol}^{1s} on the various parameters, the energy shift dependence on σ in the exact 2D and 3D limits is displayed in figure 1 for two values of a_B/R_{ex} (1 and 2). Figure 1 shows that, for a given system with given σ and a_B/R_{ex}, the energy shift is greater in the 2D case than in the 3D case. As the energy shift is, basically, a negative contribution (see equation (31)), the behaviour displayed in figure 1 tends to contribute to the increasing of the total energy when the dimension increases, a general trend that has also been shown to occur in other fractional-dimensional systems [34]. On the other hand, for a given σ and α, the system with ratio $a_B/R_{ex} = 2$ has a greater energy shift than the one with $a_B/R_{ex} = 1$ due to the fact that in the former case the coupling with the phonons (we recall that $a_B/R_{ex} \sim \hbar\omega/R_y$) is stronger. We note that a similar behaviour was found by Adamowski *et al* [40] by using a strict 3D exciton model. It is remarkable, however, that the sensitivity of this effect depends on the dimensionality. Thus, for $\alpha = 2$ the difference between the curves with $a_B/R_{ex} = 1$ and $a_B/R_{ex} = 2$ appears to be enhanced with respect to the corresponding ones in the 3D case. It is also appreciable in figure 1 that at $\sigma = 1$, as was previously discussed, the centre of mass and the centre of charge coincide, leading to a suppression of the coupling with the phonons. However, as σ decreases and m_e starts to differ from m_h, the centre of mass displaces from the centre of charge, the screening between the electron and hole becomes less effective, and the coupling with the phonons rapidly increases. Thus, roughly speaking (notice the presence of a maximum at $\sigma \neq 0$ in some of the curves), the energy shift increases as σ decreases and reaches the *bound polaron* limit at $\sigma = 0$. The presence of a maximum at $\sigma \neq 0$ in some of the curves suggests the existence of an optimal configuration for which the

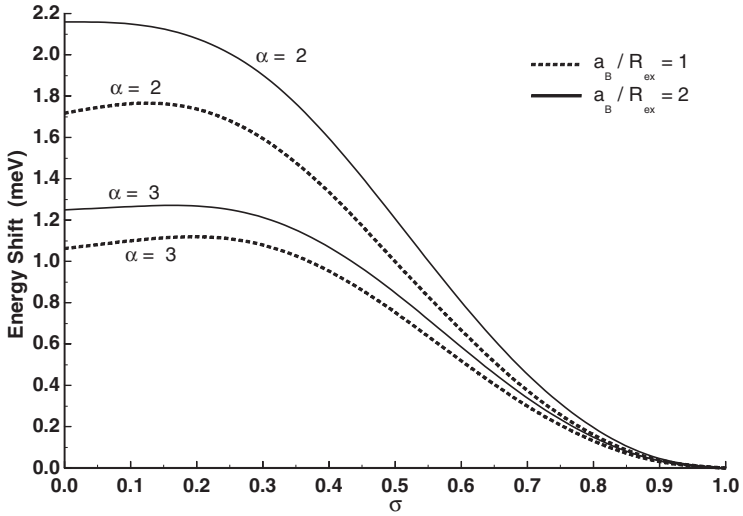

Figure 1. Energy shift (the last term in equation (31)) as a function of $\sigma = m_e^*/m_h^*$ for different values of a_B/R_{ex} and α.

coupling with the phonons becomes maximal. The study of the origin of such a configuration requires a rigorous approach involving a great variety of phonon modes and the incorporation of a realistic multisubband description of the electron–hole Coulomb interaction. As this is not a trivial procedure, the nature of optimal configuration for which the coupling with the phonons becomes maximal has not been explored in this work.

In figure 2, the mass correction $\Delta M = \frac{(M_p^* - M_{ex}^*)}{M_{ex}^*} \times 100$ is shown as a function of the dimensionality α and for different values of σ and the ratio a_B/R_{ex}. In obtaining figure 2 we have used $\eta_{ex} = 0.1$ without loss of much generality. The figure shows a gradual decrease in the mass correction with α. As for the energy shift, in the case of the mass correction the difference between the curves with different a_B/R_{ex} also increases when decreasing σ and/or α. The explanations concerning this behaviour and the other features shown in figure 2 are quite similar to that given in the discussion of the results displayed in figure 1 and we therefore omit them.

4. Excitonic polaron binding energy

The excitonic polaron binding energy can be calculated by subtracting the self-energy of the hole and electron polarons [31] from the ground state energy of the excitonic polaron (equation (31)). We then obtain the excitonic polaron binding energy as

$$E_b(\alpha) = \frac{\sqrt{\pi}}{2}\hbar\omega\left[\frac{\Gamma[\frac{\alpha_e}{2} - \frac{1}{2}]}{\Gamma[\frac{\alpha_e}{2}]}\eta_e + \frac{\Gamma[\frac{\alpha_h}{2} - \frac{1}{2}]}{\Gamma[\frac{\alpha_h}{2}]}\eta_h\right] - \eta_{ex}\hbar\omega M_1(\alpha, \gamma_e, \gamma_h) - \frac{4R_y}{(\alpha - 1)^2}, \qquad (32)$$

where α_e (α_h) is the dimensionality associated with the confined electron (hole) polaron and η_e (η_h) is the electron (hole) coupling constant which is evaluated by replacing the exciton mass by the electron (hole) mass in the expression used for η_{ex} in equation (25).

It is important to use an appropriate method for evaluating α as it is crucial to compute $E_b(\alpha)$ in equation (32). In the absence of interaction with phonons, the dimensional parameter that characterizes the degree of 'compression' of the confined exciton can be calculated in

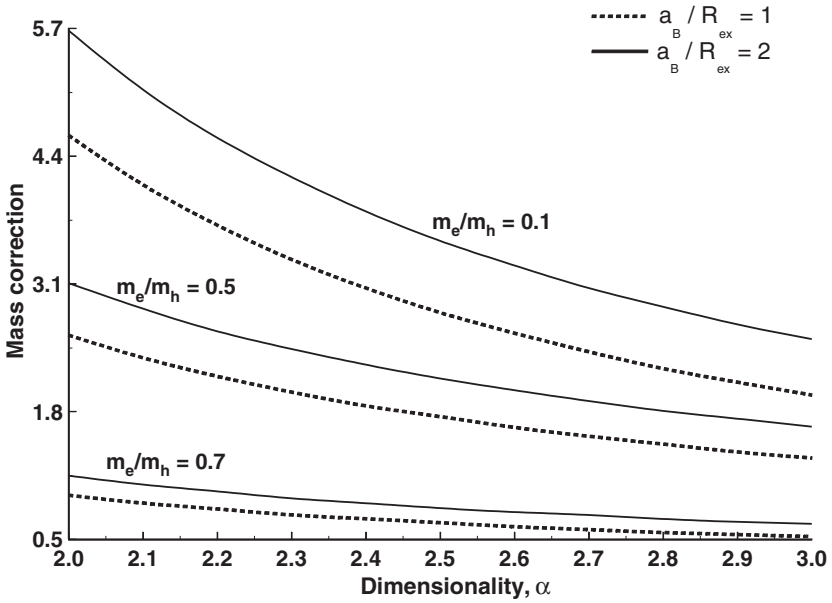

Figure 2. Mass correction $\Delta M = \frac{(M_{\rm p}^* - M_{\rm ex}^*)}{M_{\rm ex}^*} \times 100$ as a function of α for different values of σ and $a_{\rm B}/R_{\rm ex}$. $\eta_{\rm ex}$ has been taken as 0.1.

different ways (see for instance [18, 20, 21]). The easiest way to evaluate α is by using the *ansatz* [18]

$$\alpha = 3 - \exp\left(-\frac{L_{\rm w}}{2a_{\rm B}}\right), \tag{33}$$

where $L_{\rm w}$ represents the well width. The equation above is valid for infinite depth QWs, and therefore for practical purposes (real QWs have finite potential barriers) it is appropriate for large QWs only. At smaller well widths ($L_{\rm c} < L_{\rm w} < 2a_{\rm B}$, with $L_{\rm c}$ a certain critical value) some improvements can be made by replacing $a_{\rm B}$ by an effective exciton radius [41]:

$$a_{\rm B}^* = \left(\frac{a_{\rm B}^2 L_{\rm w}}{2}\right)^{1/3}. \tag{34}$$

However, in the range $L_{\rm w} < L_{\rm c}$, where tunnelling processes become important, equations (33) and (34) cannot provide accurate estimates for α because they do not take into account the spreading of the electron and hole wavefunctions into the barrier regions. In order to incorporate these effects, a generalized version of equation (33) was proposed in [18]. Although simple, the generalized expression requires the introduction of a large set of ansatz and *a priori* definitions that can be even larger if one tries to incorporate the exciton–phonon interaction effects. In order to avoid the use of heuristic definitions, we use a microscopic approach [20] that takes into account the penetration of the carriers into the barriers and incorporates the continuous interpolation of the material parameters from their values in the well region (at large well widths) to their values in the barrier regions (at very small well widths). Using the microscopic approach, which is phenomenological rather than heuristic in nature, accurate values of α can be computed through the expression

$$\alpha = 2 + \left[1 + \left(\frac{(1 - \eta_{\rm ex} M_2(\alpha, \gamma_{\rm e}, \gamma_{\rm h}))a_{\rm B}}{Z}\right)^2\right]^{-1/3}. \tag{35}$$

The quantity Z can be calculated analytically. It gives a measure of the extension of the electron–hole pair and is computed by just using the electron and hole envelope wavefunctions (for more details see [20]). It is worth noting that in equation (35) we have generalized the expression originally proposed for the case of confined excitons [20] by introducing the effects of the exciton–phonon interaction in a renormalized Bohr radius $(1-\eta_{\rm ex}M_2(\alpha,\gamma_{\rm e},\gamma_{\rm h}))a_{\rm B}$ that now replaces $a_{\rm B}$.

Although, in principle, the appropriate values of α have to be found by solving the transcendental equation (35) numerically (and this does not involve much effort), one can, however, obtain a good estimation of the dimensionality in a purely analytical way by computing a first approximation of α from equations (33) (and equation (34) for narrow QWs). The final value of the dimensionality is then obtained through equation (35), but using the first approximation of α in the evaluation of the term $M_2(\alpha,\gamma_{\rm e},\gamma_{\rm h})$.

The dimensionalities associated with the electron and hole polarons can be calculated as in [31]. For infinite QWs, expressions analogous to equation (33) can be used:

$$\alpha_{\rm e}=3-\exp\left(-\frac{L_{\rm w}}{2R_{\rm e}}\right),\qquad \alpha_{\rm h}=3-\exp\left(-\frac{L_{\rm w}}{2R_{\rm h}}\right), \tag{36}$$

where $R_{\rm e}$ ($R_{\rm h}$) is the electron (hole) polaron radius computed through the substitution of $M^*_{\rm ex}$ by the electron (hole) mass in the expression used for $R_{\rm ex}$. For more accurate estimates of $\alpha_{\rm e}$ and $\alpha_{\rm h}$, effects of the carrier penetration into the barrier regions can be incorporated by introducing an effective well width and main values of the corresponding well and barrier material parameters [31].

It is to be noted that our technique of mapping the excitonic polaron from the real system to the effective system of a fractional space refers to the physical quantities we are interested in, i.e., the excitonic polaron energy and mass. The existence of such a mapping for the case of exciton or impurities binding energies has been mathematically demonstrated (see [21, 24, 25, 27]) where the transformations lead to *unique* and *real* solutions for the dimensional parameter. However, the question arises as to how best to determine the dimensional parameter that guarantees a similar mapping for excitonic polarons. As the exact transformation for the excitonic polaron is unknown due to the unavailability of a precise and unique mapping procedure, we refer to the fractional-dimensional space approach as an approximation. In this regard, equation (35) provides an approximate generalization to equation (33), and its reliability can be easily validated by comparison with known experimental theoretical estimates (see section 6).

5. Energy difference between different excitonic polaron states

A quantity that can be of interest not only from the theoretical but also from the experimental point of view is the energy difference between excitonic polaron states. In particular the energy difference between the 1s and 2s excitonic polaron states is of special interest because it gives information about the optical properties of the system and is a quantity that can be measured in the experiments in a direct way.

Within the framework of the theory developed in section 2, the energy difference between the 1s and 2s levels of the excitonic polaron can be easily determined. The procedure for obtaining the energy of the excited states is quite similar to that used for the case of the ground state. For the 2s state we assume the fractional-dimensional exciton wavefunction [16, 32]:

$$\psi_{2s}(r)=G_{2s}(\alpha)\left(\frac{\alpha^2-1}{4}-\frac{r}{a_{\rm B}}\right)\exp\left[-\frac{2}{\alpha+1}\frac{r}{a_{\rm B}}\right], \tag{37}$$

where the factor G_{2s} can be easily determined from the corresponding normalization condition [16, 32]. Equation (37) is then used to derive an expression for the matrix element $V^{\alpha}_{2s,2s}(\mathbf{q})$ and a transformed Hamiltonian (similar to $\hat{H}^{T}$ in equation (16)) as was done in the case of the 1s state of the excitonic polaron. After some mathematical manipulations we finally obtain

$$E^{1s}_{ex-pol} - E^{2s}_{ex-pol} = \frac{16R_y}{(1-\eta_{ex}M(\alpha))}\frac{\alpha}{(\alpha^2-1)^2} + 16\eta_{ex}\frac{R_y^2}{\hbar\omega}\frac{1}{(1-\eta_{ex}M(\alpha))^2}\left[\frac{3}{8(\alpha-1)^4} - \frac{1}{(\alpha+1)^4}\right], \tag{38}$$

where $M(\alpha) = \frac{\Gamma[\frac{\alpha}{2}-\frac{1}{2}]}{8\Gamma[\frac{\alpha}{2}+1]}$. We remark that in obtaining equation (38) we have considered that both the 1s and 2s states are characterized by the same value of the dimensionality. In practice, however, different states are not strictly characterized by the same dimensionality. As the dimensionality constitutes a measure of the degree of compression of the exciton wavefunction, a variation of the well width or in the height of the barriers will induce changes in the confinement and, consequently, a variation in the value of the dimensionality. In a similar way, as different states posses different geometries and extensions, one can expect that they will *feel* the confinement in different manners [21]. Therefore, what happens is, strictly speaking, that each state is characterized by a particular value of the dimensionality [21]. Nevertheless, for the case of the energy difference between the 1s and 2s states one still can obtain a good estimation of $E^{1s}_{ex-pol} - E^{2s}_{ex-pol}$ by assuming the same value of α for both states [18]. The results computed by using equation (38) will be discussed in the next section.

Another quantity that can be of general interest is the so-called phonon Lamb shift (i.e., the enhancement of the excitonic polaron energy of the excited 2s state with respect to the 2p state [42]). For the computation of the matrix element $V^{\alpha}_{2p,2p}(\mathbf{q})$ we use the fractional-dimensional wavefunction corresponding to the 2p exciton state [16, 32]:

$$\psi_{2p}(r) = G_{2p}(\alpha)\frac{r}{a_B}\exp\left[-\frac{2}{\alpha+1}\frac{r}{a_B}\right]\cos\theta, \tag{39}$$

where $G_{2p}(\alpha)$ is a normalization factor [16, 32]. After some mathematical manipulations we finally obtain an expression for the Lamb shift of the excitonic polaron:

$$E^{2p}_{ex-pol} - E^{2s}_{ex-pol} = \frac{64\eta_{ex}}{5(\alpha+1)^4}\frac{R_y^2}{\hbar\omega}\frac{1}{(1-\eta_{ex}M(\alpha))^2}. \tag{40}$$

In figure 3 we have plotted the phonon Lamb shift as a function of the dimensionality α for different values of the coupling constant $\eta_{ex} = 0.5$, 0.7 and 0.9. We have assumed $R_y^2/\hbar\omega \approx 1$ meV in order to gain some insight into the dependence of the Lamb shift on α and η_{ex}. The figure shows that the Lamb shift decreases as α increases, and that the rate of this trend is faster at higher values of the exciton coupling constant. One can also appreciate from figure 3 that the smaller the exciton coupling constant the smaller the phonon Lamb shift. Thus, for instance, in the case of GaAs/$Ga_{1-x}Al_xAs$ QWs, where $\eta_{ex} \leqslant 0.1$, the Lamb shift becomes too small (even in the 2D limit) to be detected experimentally by current instruments.

Finally, we want to remark that in order to obtain analytical solutions (see equations (38) and (40)), we have assumed an exciton of large radius ($\geqslant$100 Å) and binding energy that is less than the phonon energy, i.e., $R_y \leqslant \hbar\omega$. Details of calculations of a thorough study, where a wider range of materials can be considered, are rather lengthy and will be given elsewhere.

6. Comparison with experimental results

In figure 4 we show our fractional-dimensional results (solid curves) for the excitonic polaron binding energy as a function of the well width and for different values of the Cd concentration x

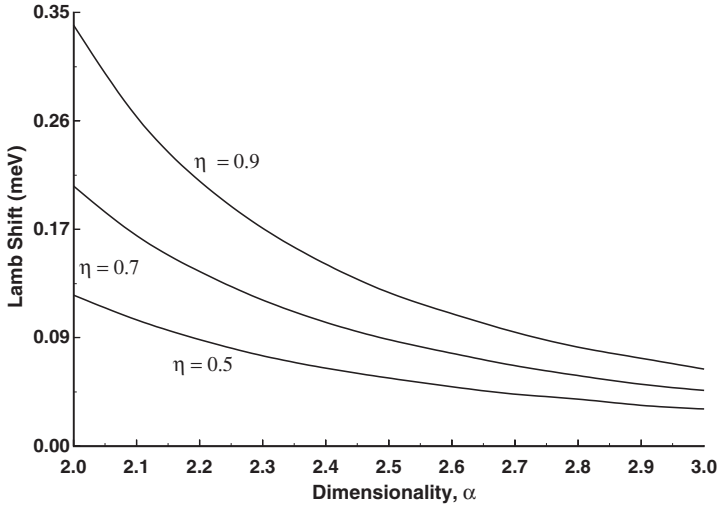

Figure 3. Phonon Lamb shift as a function of the dimensionality α for different values of the coupling constant η_{ex}.

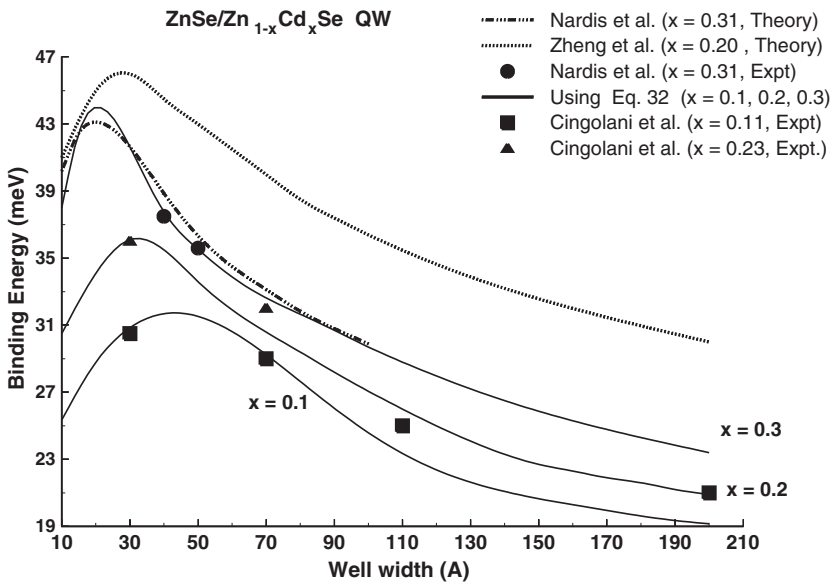

Figure 4. Well width dependence of the excitonic polaron binding energy in $ZnSe/Zn_{1-x}Cd_xSe$ QWs. Solid curves represent the results of our calculations performed through equations (32), (35), and (36) and assuming the same material parameters as in [14] (for $x = 0.3$) and [15] (for $x = 0.2$, 0.1). Experimental results from [14] and [15] are denoted by solid symbols and the variational calculations by Nardis *et al* [14] and by Zheng *et al* [13] are denoted by dashed–dotted and dotted curves, respectively.

(0.1, 0.2 and 0.3) in $ZnSe/Zn_{1-x}Cd_xSe$ QWs. Our results were computed using equations (32), (35) and (36) and material parameters as defined by Nardis *et al* [14] (for the case $x = 0.3$) and Cingolani *et al* [15] (for the cases $x = 0.2, 0.1$). Theoretical results obtained by Zheng *et al* [13] and by Nardis *et al* [14] (dotted and dashed–dotted curves, respectively) as well as experimental results (solid symbols) reported by Nardis *et al* [14] and Cingolani *et al*

Table 1. Comparison of exciton binding energies (meV) at $\alpha = 2$ (exact 2D) and $\alpha = 3$ (bulk).

	$\alpha = 2$			
	Equation (32)	Reference [47]	Equation (32)	Expt.
CdTe	46.2	45.96	11.5	11[b]
CdS[a]	140.7	—	27	30[b]
CuCl	655	656.3	140	190[c]
TlCl[a]	74.8	—	12	11[d]
TlBr[a]	45	—	9	6[d]

[a] Exact 2D binding energies are not available for CdS, TlCl and TlBr in [47].
[b] Experimental result from [48].
[c] Experimental result from [49].
[d] Experimental result from [50].

[15] are also included in the figure. The good overall agreement between our results and the experimental ones is quite apparent, especially in the region of strong confinement. As was mentioned in section 2, we expect our approximation to be valid in the weak to intermediate coupling regimes. Therefore, as the phonon coupling becomes strong the application of the proposed approach can be, in principle, questionable and its accuracy decreases. This effect is, however, somewhat minimized when considering systems with large Rydberg and strong confinement. In the strong confinement regime the exciton binding energy (without phonon effects) increases very quickly in comparison with the polaronic corrections and for materials with large Rydberg the exciton binding energy becomes (without phonon effects) considerably large, so that in that case one can expect that even the strong phonon coupling regime could be treated within perturbation theory. For the case of weak confinement and strong phonon coupling, however, this situation is no longer true, and the accuracy of our calculations rapidly decreases, as can be clearly seen from figure 4 in the region of large well widths or by comparing the results shown in table 1 for $\alpha = 2$ (strong confinement) and $\alpha = 3$ (no confinement).

As expected, the spreading of the electron and hole wavefunctions into the barrier regions at very small well widths ($L_w \leqslant 30$ Å) results in a peak in the binding energy at some critical well width at which the confinement is maximal and the dimensionality α reaches its minimal value. The figure also shows that as the Cd concentration x increases the excitonic polaron binding energy increases. This behaviour is easily explained by the fact that a deeper well (at larger x values) confines the exciton more efficiently, the exciton dimensionality becomes smaller, and the binding turns stronger.

The fractional-dimensional excitonic polaron binding energy and the energy difference between the 1s and 2s excitonic polaron states as functions of the GaAs/$Ga_{0.7}Al_{0.3}As$ QW width are represented by solid lines in figures 5 and 6, respectively. In both cases the corresponding dimensionalities α, α_e and α_h needed in the evaluation of equations (32) and (38) were computed using equations (35) and (36) and the same material parameters as used by Oelgart *et al* [43]. As can be clearly appreciated in figure 5, our theoretical estimates of the heavy-hole excitonic polaron binding energy are in good agreement with theoretical and experimental results reported by Oelgart *et al* [43] and Petrou *et al* [44]. In figure 6 we have included, for comparison, experimental values of the energy difference between the 1s and 2s heavy-hole exciton states obtained by Oelgart *et al* [43], Dawson *et al* [45] and Koteles *et al* [46]. Again, the overall agreement between our fractional-dimensional results and previously reported experimental data is quite apparent. It is worth noting that our results displayed in figure 6 were calculated by approximating the dimensionality α_{2s} that characterizes the 2s exciton state by the same value of the dimensionality α that characterizes the 1s exciton state,

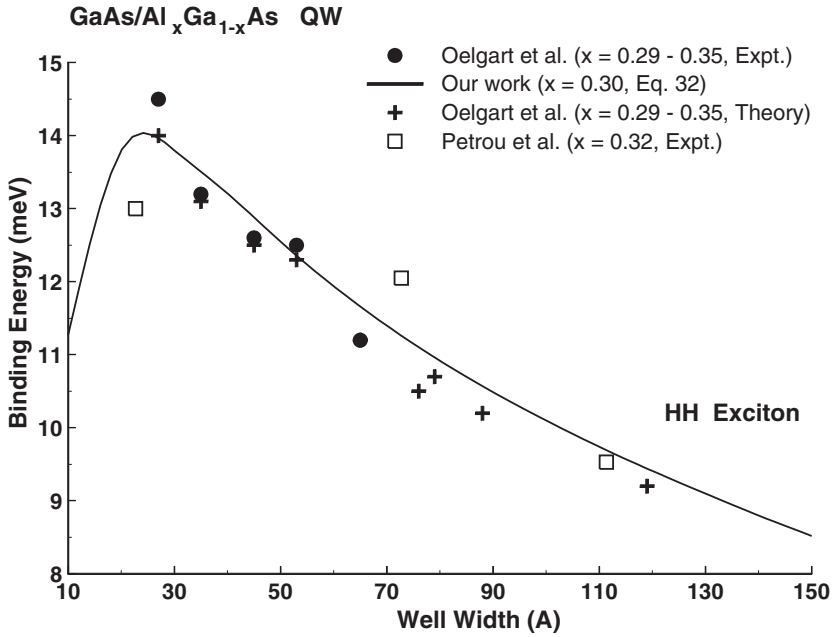

Figure 5. Well width dependence of the excitonic polaron binding energy in $GaAs/Al_xGa_{1-x}As$ QWs. Solid dots and crosses are, respectively, experimental and calculated binding energies reported by Oelgart *et al* [43] for $x = 0.29$–0.35. The solid curve corresponds to our calculations using equation (32) and the same parameters as defined by Oelgart *et al* [43]. Symbols represented by a hollow box correspond to experimental results of Petrou *et al* [44] obtained for $x = 0.32$.

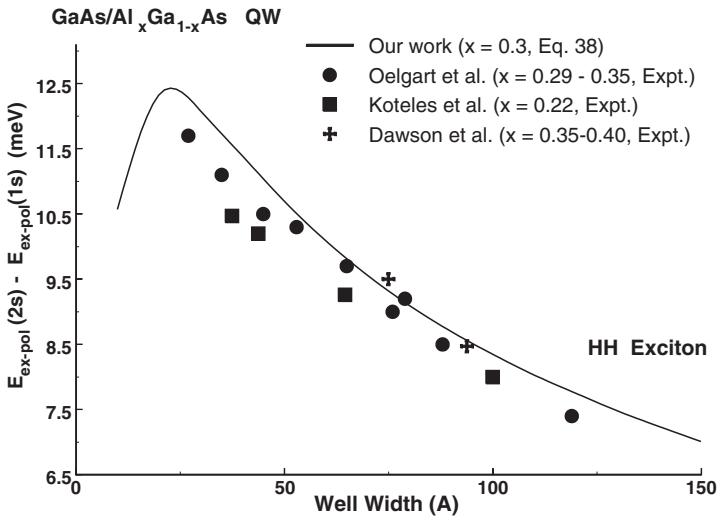

Figure 6. Energy difference between the 1s and 2s states of the heavy-hole excitonic polaron in $GaAs/Al_xGa_{1-x}As$ QWs as a function of the well width. The solid curve corresponds to our theoretical result evaluated using equations (38) and (35) and the same material parameters as in [43]. The figure includes experimental results of Oelgart *et al* [43] (solid circles), Dawson *et al* [45] (crosses) and Koteles *et al* [46] (solid squares).

i.e., we assumed that $\alpha_{2s} = \alpha$. As was previously discussed in section 5, however, to different states correspond, strictly speaking, different dimensionalities. Actually, for narrow QWs, as

Table 2. Material Parameters.

	m_e^*	m_h^*	ε_0	ε_∞	$\hbar\omega$	η_e	η_h	η_{ex}	a_B (Å)	R_{pol} (Å)	R_{ex} (Å)	R_y (meV)
CdTe[a]	0.088	0.60	10.3	6.9	20.7	0.364	0.950	1.02	48	46	16.4	9
CdS[b]	0.18	0.70	9.7	5.2	38	1.59	0.718	1.415	24	24	11	39
CuCl[a]	0.40	3.60	7.4	3.7	27.2	1.911	5.733	6.04	5.2	20	6	178
TlCl[c]	0.31	1.32	37.6	5.1	21.5	5.442	2.4	4.9	50	39	17	13.1
TlBr[c]	0.19	0.95	35.1	5.4	14.3	5.16	2.1	4.17	46	49	20	9

[a] First seven parameters taken from [47].
[b] First five parameters taken from [11].
[c] First five parameters taken from [50].

the 2s state has a spatial extension that is, in principle, larger than the 1s state extension, it *feels* the confinement in a stronger way and is more 'compressed' by the QW barrier [21]. Therefore, in the region of narrow QWs $\alpha_{2s} < \alpha$ [21]. On the other hand, taking into account that the exciton energy increases as the dimension increases (recall that on increasing the dimensionality, the binding energy decreases, and as it contributes negatively to the total energy, the total energy increases with the dimension) one can conclude that in the region of narrow QWs the value of the energy E^{2s}_{ex-pol} at α is, actually, greater than its corresponding value at α_{2s}. Consequently, in the narrow wells region the here assumed approximation $\alpha_{2s} \approx \alpha$ produces a certain overestimation in our calculation of the energy difference $E^{2s}_{ex-pol} - E^{1s}_{ex-pol}$. One can then expect that our results in figure 6 can still be improved, especially in the region of narrow wells, if a more realistic value of α_{2s} is incorporated in our theoretical approach. However, a better estimation of α_{2s} in a simple way remains a challenge. No heuristic or macroscopic formulations for the calculation of α_{2s} are yet known, and the generalization of the systematic method developed in [21] to the case of excitonic polarons is not a trivial task.

The excitonic polaron binding energy evaluated for a variety of materials in the exact 2D and 3D limits is shown in table 1, together with theoretical and experimental results reported by other authors. Again, an overall agreement between our results and those reported in [47–50] can be clearly appreciated. The material parameters we used in evaluating the excitonic polaron binding energies reported in table 1 are given in table 2. It should be noted that in table 2, in the cases of CdS, CuCl, TlCl, and TlBr, the corresponding effective Rydbergs were calculated by using $R_y = R_y^\infty \frac{\varepsilon_\infty}{(\varepsilon_\infty - \varepsilon_0)} + R_y^0 \frac{\varepsilon_0}{(\varepsilon_\infty - \varepsilon_0)}$, where R_y^0 and R_y^∞ are the Rydberg energies obtained with ε_0 and ε_∞, respectively.

It is to be noted that we have applied the fractional-dimensional space formalism within the framework of a perturbative method which approximates exciton–phonon systems between the weak to intermediate coupling range quite well. Figure 4 as well as table 1 show good agreement between our theoretical results and II–VI and I–VII compound systems which are known not to have weak exciton–phonon coupling. It is interesting to note that the agreement between experimental and theoretical results is best for excitonic systems where the polaron radius (R_{pol}) is of the same order as the exciton Bohr radius (table 2). In fact, the closeness of the two radii highlights the magnitude of interplay between the electron–hole potential and electron–phonon interaction [51] and suggests that transitions between the different internal exciton state will have an influence in its polaronic corrections. However, consideration of such transitions requires the incorporation of a full three-dimensional multisubband description of the electron–hole Coulomb interaction. This is not a trivial procedure and is therefore beyond the scope of this paper. Our approximation, however, allows us to derive completely analytical results for excitonic polarons which can be generalized to other models like the double quantum wells and quantum disc systems.

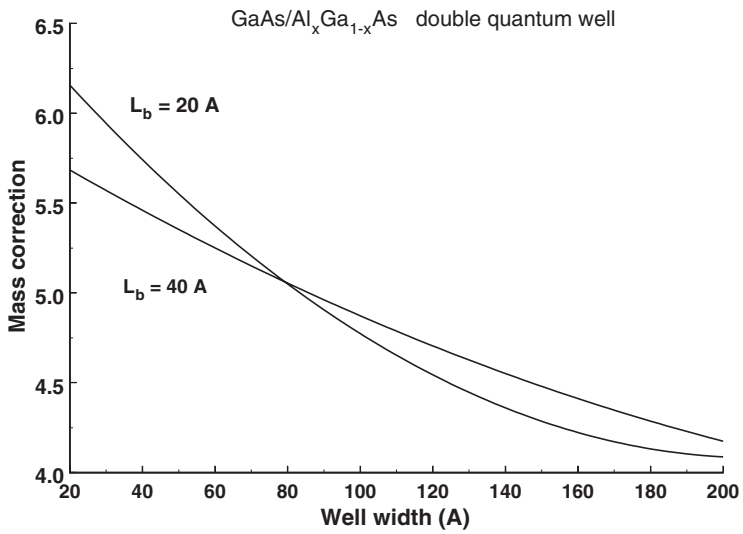

Figure 7. Polaronic mass correction $\Delta M = \frac{(M_{\rm p}^* - M_{\rm ex}^*)}{M_{\rm ex}^*} \times 100$ as a function of the well width in GaAs/$Al_{0.3}Ga_{0.7}$As SCDQW at fixed barrier thicknesses (20 and 40 Å).

The good quantitative agreement in table 1 suggests that changes in polaronic corrections due to the neglect of a component, $\hat{H}_I'$, of the interaction operator in equation (16) may be offset by the changes arising due to neglect of transitions involving internal exciton states mentioned in the previous paragraph. Moreover, the effect of particle–phonon interactions on the excitonic polaron is expected to introduce changes that are not expected to affect the order of magnitude of polaron parameters like energy shift and effective mass quantities (as is evident in figures 4, 5 and table 1). Hence the overall pertinent features of the excitonic polaron system remains intact in low-dimensional systems in spite of the assumption that we have used in this work and which appears well justified for a wide range of material systems. The derivation of analytical solutions, however, remains a challenge for alternative methods [7, 9] known to be theoretically valid for all ranges of the coupling. This is mainly due to the increased complexity of mathematically transforming the composite exciton–phonon system into an effective fractional-dimensional space.

7. Coupled double quantum wells

The problem of excitonic polarons in coupled double quantum wells (CDQW) [52], in which two coupled wells are separated by a barrier material of width, $L_{\rm b}$, is complex. This is mainly due to the number of matching conditions that have to be considered at the interfaces for both excitons and phonons. However, the properties of the special case of a symmetric coupled quantum well (SCDQW) system in which the widths of the adjacent quantum wells are equal can be studied using the fractional-dimensional space formalism.

In figure 7, we have evaluated the polaronic mass correction $\Delta M = \frac{(M_{\rm p}^* - M_{\rm ex}^*)}{M_{\rm ex}^*} \times 100$ as a function of the well width in GaAs/$Al_{0.3}Ga_{0.7}$As SCDQW at fixed barrier thicknesses (20 and 40 Å). We have used the values of α calculated [52] at various well widths and for fixed barrier widths (20 and 40 Å), as well as equations (29), (30) and (35) and material parameters as given in [52]. The effect of the barrier material on the polaronic properties is notable. For narrow

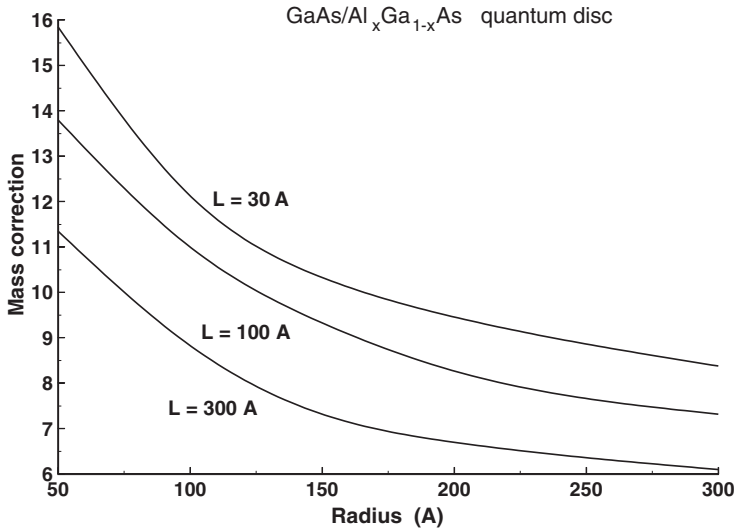

Figure 8. Polaronic mass correction $\Delta M = \frac{(M_{\rm p}^{*} - M_{\rm ex}^{*})}{M_{\rm ex}^{*}} \times 100$ as a function of the disc radius, R, at lengths, $L = 30$, 100 and 300 Å in GaAs/$Al_{0.3}Ga_{0.7}$As quantum discs.

barrier and wells, there is a higher integrated probability of finding the charge carriers in the well region, and thus the excitonic polaron wavefunction is mainly localized in the well regions. Then, as the barrier width increases (i.e., the spatial separation between the wells increases) the spreading of the excitonic wavefunction and the excitonic radius increases, leading to a decrease of the confinement effects and, consequently, to a decrease of the polaronic effects (see the region of narrow wells in figure 7). This trend is, however, reversed as the well width increases. When the well widths approximate the value of the excitonic radius, the exciton localizes in one of the wells and is more efficiently confined for wider barriers (see the region of wide wells in figure 7). It is to be noted that a similar trend as given in figure 7 is observed for the energy shift (see equation (31)) for various well widths at fixed barrier thickness.

Another feature of interest is the effect of the barrier width on the phonon Lamb shift (see equation (40)) in coupled double quantum wells. With the inverse dependence of the Lamb shift on the dimensionality, a plot of the Lamb shift versus the well width at different barrier widths is predicted to show a crossover at some critical well width, depending on the well and barrier material parameters (e.g., aluminium concentration x, effective masses of charge carriers).

8. Quantum discs and self-trapping effects

By varying the radius, R, and length, L, of the quantum disc, one can explore properties in the limiting situations of the excitonic polaron in bulk ($R, L \gg a_{\rm B}$), the quantum well ($R \gg a_{\rm B}$, $L \leqslant a_{\rm B}$), the quantum wire ($R \leqslant a_{\rm B}$, $L \gg a_{\rm B}$) and the quantum dot ($R, L \leqslant a_{\rm B}$). Recently, Tong *et al* [53] performed variational calculations of the exciton binding energies in the intermediate range of values for R and L in GaAs/$Ga_{0.7}Al_{0.3}$As material systems. Using an expression similar to the last term given in equation (3), estimates of the exciton dimensionality for various values of R and L in GaAs/$Al_{0.3}Ga_{0.7}$As quantum discs were obtained by Tong *et al* [53]. While such a method of estimating exciton dimensionalities is questionable near the limit of the quantum dot, we considered values outside this range and obtained in figure 8

the polaronic mass correction as a function of the disc radius, R, at lengths, $L = 30$, 100 and 300 Å in GaAs/$Al_{0.3}Ga_{0.7}$As quantum discs. The mass correction values were calculated using equations (29), (30) and (35) and the material parameters given in [53]. Although the results shown in figure 8 are consistent with our intuitive expectation, the rapid rise in mass correction with the decrease in L and R is notable. Under this situation, the excitonic polaron can be considered as being self-trapped and localized as a result of its interaction with optical phonons. Using the fact that the excitonic polaron energy, $E^{1s}_{ex-pol} \leqslant 0$ (equation (31)) when self-trapping occurs, we estimate, using the material parameters in [53], that exciton trapping due to optical phonons becomes important for exciton dimensionalities, $\alpha \leqslant 1.2$. Using a similar approach, we estimate $\alpha \leqslant 1.8$ for self-trapping effects to be observed in CdTe-based confined systems.

It is interesting to compare our predictions with the results of Jacak *et al* [54], who recently evaluated energy shifts of the order of a few millielectronvolts of the exciton interacting with optical phonons in InAs/GaAs dots. Using equation (31), we have computed energy shifts in the range 5–10 meV for excitonic polarons in InAs/GaAs based confined systems of dimensionalities 1.5–2.0. The energy shift increases rapidly beyond 10 meV for $\alpha \leqslant 1.4$, implying that significant shifts in the excitonic spectrum are expected to be observed in the true quantum dot region.

9. Conclusions

In summary, we have extended the fractional-dimensional space approach, in which the real confined heterostructured system is mapped into an effective fractional-dimensional bulk-like environment, to the study of ground and excited excitonic polaron states in confined systems. This approach is motivated by the fact that the relative motion of an excitonic polaron cannot be considered exactly two or three dimensional but possibly of an intermediate dimension in quantum wells. We have also proposed a microscopic definition which incorporates the penetration of the electron and hole wavefunctions into the barrier regions and the effects of the exciton–phonon interaction to determine the effective dimensionality that describes the degree of compression of the confined excitonic polaron system.

The excitonic polaron problem in nanostructures is a complicated problem that, within the standard procedures, requires extensive computational efforts. Through the derivation of analytical results, our results can be of considerable help for experimentalists as well as theoreticians when rapid and accurate estimates of the excitonic polaron corrections are needed. Thus, the proposed method does not intend to compete with the standard methods (that are specially needed if detailed and extensive studies are required) but allows convenient estimation of the effective mass and the ground state energy of an excitonic polaron in a confined system. We have also obtained explicit analytical expressions for the energy difference between the 1s and 2s states as well as the Lamb shift corresponding to the confined excitonic polaron. Calculations performed for a wide variety of material systems show good agreement with previous theoretical estimates and available experimental measurements, and provide new theoretical predictions in the coupled double quantum well and quantum disc systems. Even though we have restricted our model systems to cases where the dimensionality α is less than 3, the work done here can be extended to indirect excitons and impurities located in the central barrier of a double quantum well where $\alpha \geqslant 3$. In conclusion, our developed formalism provides a simple, general, and comprehensive picture of the excitonic polarons in confined systems.

References

[1] Weisbuch C and Vinter B 1991 *Quantum Semiconductor Structures* (Boston, MA: Academic)
[2] Bayer M, Hawrylak P, Hinzer K, Fafard S, Korkusinski M, Wasilewski Z R, Stern O and Forchel A 2001 *Science* **291** 451
[3] Haug H and Koch S W 1993 *Quantum Theory of the Optical and Electronic Properties of Semiconductors* (Singapore: World Scientific)
[4] Chemla D S 1999 *Ultrafast Transient Nonlinear Optical Processes in Semiconductors* ed R K Willardson and E R Weber (New York: Academic) p 175
[5] Landau L D 1933 *Sov. Phys.* **3** 664
[6] Kuper C G and Whitfield G D 1963 *Polarons and Excitons* (Edinburgh: Oliver and Boyd)
[7] Feynman R P 1955 *Phys. Rev.* **97** 660
[8] Devreese J T 1996 *Polarons, Encyclopedia of Applied Physics* (Trigg: VHC Publishers) p 383
[9] Prokof'ev N V and Svistunov B V 1998 *Phys. Rev. Lett.* **81** 2514
[10] Alexandrov A S and Mott N F 1994 *Rep. Prog. Phys.* **57** 1197
[11] Pollmann J and Buttner H 1975 *Solid State Commun.* **17** 1171
[12] Iadonisi G, Bassani F and Strinati G 1989 *Phys. Status Solidi* b **153** 611
[13] Zheng R, Matsuura M, Fujimoto M, Yamada Y and Taguchi T 1999 *Japan. J. Appl. Phys.* **38** 808
[14] De Nardis A, Pellegrini V, Colombelli R, Beltram F, Vanzetti L, Franciosi A, Krivorotov I N and Bajaj K K 2000 *Phys. Rev.* B **61** 1700
[15] Cingolani R, Prete P, Greco D, Giugno P V, Lomascolo M, Rinaldi R, Calcagnile L, Vanzetti L, Sorba L and Franciosi A 1995 *Phys. Rev.* B **51** 5117
[16] Stillinger F H 1977 *J. Math. Phys.* **18** 1224
[17] He X F 1991 *Phys. Rev.* B **43** 2063
[18] Mathieu H, Lefebvre P and Christol P 1992 *Phys. Rev.* B **46** 4092
[19] Lefebvre P, Christol P and Mathieu H 1993 *Phys. Rev.* B **48** 17308
[20] Christol P, Lefebvre P and Mathieu H 1993 *J. Appl. Phys.* **74** 5626
[21] Matos-Abiague A, Oliveira L E and de Dios-Leyva M 1998 *Phys. Rev.* B **58** 4072
[22] Andreani L C and Pasquarello A 1990 *Phys. Rev.* B **42** 8928
[23] Thilagam A 1999 *Phys. Rev.* B **59** 3027
[24] Matos-Abiague A, Oliveira L E and de Dios-Leyva M 2001 *Physica* B **296** 342
[25] Mikhailov I D, Betancur F J, Escorcia R A and Sierra-Ortega J 2003 *Phys. Rev.* B **67** 115317
[26] Zhao Q X, Monemar B, Holtz P O, Willander M, Fimland B O and Johannessen K 1994 *Phys. Rev.* B **50** 4476
[27] Reyes-Gómez E, Matos-Abiague A, Perdomo-Leiva C A, de Dios-Leyva M and Oliveira L E 2000 *Phys. Rev.* B **61** 13104
[28] Thilagam A 1997 *Phys. Rev.* B **56** 4665
[29] Tanguy C, Lefebvre P, Mathieu H and Elliot R J 1997 *J. Appl. Phys.* **82** 798
[30] Thilagam A 2001 *Phys. Rev.* B **63** 45321
[31] Matos-Abiague A 2002 *Phys. Rev.* B **65** 165321
[32] Thilagam A 1997 *Phys. Rev.* B **56** 9798
[33] Thilagam A 1999 *Opt. Quantum Electron.* **31** 405
[34] Matos-Abiague A 2001 *J. Phys. A: Math. Gen.* **34** 11059
[35] Bak Z 2003 *Phys. Rev.* B **68** 64511
[36] Lee T D, Low F and Pines D 1953 *Phys. Rev.* **90** 297
[37] Oh I K, Singh J, Thilagam A and Vengurlekar A S 2000 *Phys. Rev.* B **62** 2045
[38] Zwillinger D 1992 *Handbook of Integration* (Boston, MA: Jones and Bartlett) p 53
[39] Exton H 1978 *Handbook of Hypergeometric Integrals* (Chichester: Ellis-Horwood)
[40] Adamowski J, Gerlach B and Leschke H 1981 *Phys. Rev.* B **23** 2943
[41] Hrivnak L 1992 *J. Appl. Phys.* **72** 3218
[42] Mitra T K, Chatterjee A and Mukhopadhyay S 1987 *Phys. Rep.* **153** 91
[43] Oelgart G, Proctor M, Martin D, Morier-Genaud F, Reinhart F K, Orschel B, Andreani L C and Rhan H 1994 *Phys. Rev.* B **49** 10456
[44] Petrou A, Waytena G, Liu X, Ralston J and Wicks G 1986 *Phys. Rev.* B **34** 7436
[45] Dawson P, Moore K J, Duggan G, Ralph H I and Foxon C T 1987 *Phys. Rev.* B **34** 6007
[46] Koteles E S and Chi J Y 1988 *Phys. Rev.* B **37** 6332
[47] Geddo M and Iadonisi G 1990 *Nuovo Cimento* D **12** 164
[48] Segall B and Marple D T F 1967 *Physics and Chemistry of II–VI Compounds* ed M Aven and J Prener (Amsterdam: North-Holland)

[49] Lewonczuk S, Ringeisen J and Nikitine N 1972 *J. Physique* **32** 941
[50] Bachrach R Z and Brown F C 1970 *Phys. Rev.* B **1** 818
[51] Gerlach B, Wusthoff J and Smondyrev M A 1999 *Phys. Rev.* B **60** 16569
[52] Matos-Abiague A, Oliveira L E and de Dios-Leyva M 2000 *J. Phys.: Condens. Matter* **12** 5691
[53] Koh T S, Feng Y O, Xu X and Spector H N 2001 *J. Phys.: Condens. Matter* **13** 1485
[54] Jacak L, Janutka A, Machnikowski P and Radosz A 2002 On exciton decoherence in quantum dots *Preprint* cond-mat/0212057